Rapid shift and millennial-scale variations in Holocene North Pacific Intermediate Water ventilation

Lester Lembke-Jene[a,1], Ralf Tiedemann[a], Dirk Nürnberg[b], Xun Gong[a], and Gerrit Lohmann[a]

[a]Alfred-Wegener-Institut Helmholtz-Zentrum für Polar- und Meeresforschung, 27570 Bremerhaven, Germany; and [b]GEOMAR Helmholtz-Zentrum für Ozeanforschung Kiel, 24148 Kiel, Germany

Edited by Mark H. Thiemens, University of California, San Diego, La Jolla, CA, and approved March 22, 2018 (received for review September 8, 2017)

The Pacific hosts the largest oxygen minimum zones (OMZs) in the world ocean, which are thought to intensify and expand under future climate change, with significant consequences for marine ecosystems, biogeochemical cycles, and fisheries. At present, no deep ventilation occurs in the North Pacific due to a persistent halocline, but relatively better-oxygenated subsurface North Pacific Intermediate Water (NPIW) mitigates OMZ development in lower latitudes. Over the past decades, instrumental data show decreasing oxygenation in NPIW; however, long-term variations in middepth ventilation are potentially large, obscuring anthropogenic influences against millennial-scale natural background shifts. Here, we use paleoceanographic proxy evidence from the Okhotsk Sea, the foremost North Pacific ventilation region, to show that its modern oxygenated pattern is a relatively recent feature, with little to no ventilation before six thousand years ago, constituting an apparent Early–Middle Holocene (EMH) threshold or "tipping point." Complementary paleomodeling results likewise indicate a warmer, saltier EMH NPIW, different from its modern conditions. During the EMH, the Okhotsk Sea switched from a modern oxygenation source to a sink, through a combination of sea ice loss, higher water temperatures, and remineralization rates, inhibiting ventilation. We estimate a strongly decreased EMH NPIW oxygenation of ∼30 to 50%, and increased middepth Pacific nutrient concentrations and carbon storage. Our results (*i*) imply that under past or future warmer-than-present conditions, oceanic biogeochemical feedback mechanisms may change or even switch direction, and (*ii*) provide constraints on the high-latitude North Pacific's influence on mesopelagic ventilation dynamics, with consequences for large oceanic regions.

North Pacific | intermediate water | oxygen minimum zone | stable isotopes | Holocene

Intermediate waters in the subarctic North Pacific marginal seas play a critical role in supplying oxygen (O_2) to the North Pacific oxygen minimum zone (OMZ) (1). Recent studies point to decreasing O_2 and increasing temperatures of the mesopelagic North Pacific over the past decades (2, 3). The cause of these changes, however, is hard to unambiguously attribute to either anthropogenic influences or long-term natural variability, as the latter occurs on timescales beyond the reach of instrumental datasets. One decisive factor that today prevents the development of more widespread hypoxia is the supply of dissolved O_2 to the mesopelagic water layer via ventilation of subarctic waters (1, 4). In the North Pacific, no ventilation of deep waters occurs (5) due to the existence of a strong halocline, and ventilation of intermediate water is restricted to the marginal seas, as middepth density layers do not outcrop in the open surface ocean (6, 7) (Fig. 1 and *SI Appendix*, Fig. S1). Today, the Okhotsk Sea constitutes the most important region with active ventilation during the wintertime sea ice season, when polynyas open up on the northeastern shelf areas and dense, O_2-enriched water masses form through brine rejection (8). Subsequently exported to the open North Pacific as Okhotsk Sea Intermediate Water (OSIW), they ventilate the middepth North Pacific (9) and prevent mesopelagic hypoxia occurrence (10–12). As the Okhotsk Sea is a unique region in being the world ocean's lowermost latitude where seasonal sea ice occurs, it responds with high sensitivity to changes in climate forcing, with short response times (13). Previous works have been mostly limited to OSIW and North Pacific Intermediate Water (NPIW) changes during recent glacial periods (14, 15). Few studies have addressed paleoenvironmental changes in the Okhotsk Sea over warm episodes such as the Holocene (16, 17). Here, we present high-resolution proxy records for Holocene changes in OSIW ventilation, using stable carbon isotope ratios of the epibenthic foraminifer *Cibicidoides mundulus*, a species that reliably records the $\delta^{13}C$ of $\sum CO_2$ of surrounding bottom water masses (18). Based on our records, we estimate past changes in ventilation and corresponding oxygenation of middepth Pacific water masses during the last 12 ka, with a particular focus on the warmer-than-present Early–Middle Holocene (EMH).

Results and Discussion

We used a suite of four sediment cores to reconstruct OSIW ventilation (for details, see *SI Appendix*, *Site Selection – Material and Methods* and Figs. S4 and S5). Gravity core 108 was retrieved from the western Kamchatka continental margin (52°01.330′ N, 153°35.006′ E; 627 m water depth) in the pathway of inflowing North Pacific water to the formation region of OSIW on the northeastern Okhotsk Sea continental shelf. This core thus records the precursor water mass—Western Subarctic Pacific Water (WSAPW)—delivered via the East Kamchatka Current (Fig. 1). Three sites record changes in newly formed OSIW on the eastern Sakhalin continental margin, along the export pathway into the North Pacific. Site 78 (52°40.388′ N, 144°42.203′ E; 673 m water depth) and site 4 (51°08.475′ N, 145°18.582′ E, 674 m water depth) are located within the core layer of OSIW (19, 20). Site 79

Significance

The North Pacific hosts extensive oxygen minimum zones. Ventilation of North Pacific Intermediate Water mitigates hypoxia in thermocline waters not under influence of ocean–atmosphere processes. Instrumental datasets show recent decadal decreases in O_2, but millennial-scale natural variations in mesopelagic ventilation might be large and are not understood well. We reconstruct Holocene ventilation changes in a key region (Okhotsk Sea). Modern ventilation and O_2 levels are a relatively recent feature. In the warmer-than-present Early Holocene, middepth O_2 concentrations were 25 to 50% reduced, with significant millennial-scale variations. A sudden ventilation decrease six thousand years ago is linked to higher ocean temperatures, sea ice loss, and higher remineralization, corroborated by results from paleoclimate modeling, providing constraints for future warming scenarios.

Author contributions: L.L.-J., R.T., and D.N. designed research; L.L.-J., X.G., and G.L. performed research; L.L.-J., R.T., D.N., X.G., and G.L. analyzed data; and L.L.-J. wrote the paper.

The authors declare no conflict of interest.

This article is a PNAS Direct Submission.

[1]To whom correspondence should be addressed. Email: lester.lembke-jene@awi.de.

This article contains supporting information online at www.pnas.org/lookup/suppl/doi:10.1073/pnas.1714754115/-/DCSupplemental.

Published online May 7, 2018.

EARTH, ATMOSPHERIC, AND PLANETARY SCIENCES

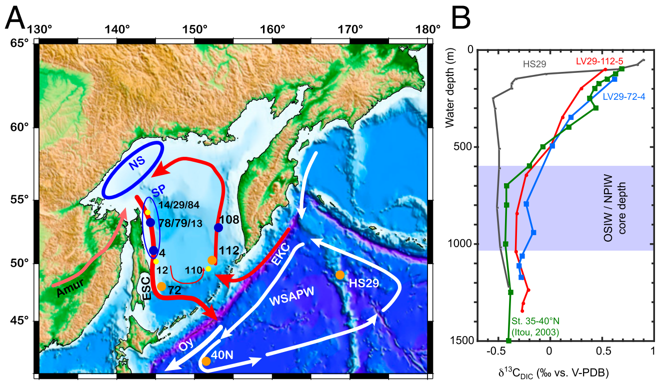

Fig. 1. Study area and regional oceanographic characteristics. (*A*) Bathymetric map with site locations. EKC, East Kamchatka Current; ESC, East Sakhalin Current; NS, Northern Shelf Polynia; Oy, Oyashio; SP, Sakhalin Polynia. (*B*) Vertical profiles of modern water $\delta^{13}C_{DIC}$ for the Okhotsk Sea and North Pacific. Station HS29 (black, open circles) records WSAPW before it enters the Okhotsk Sea (14); Station 112 represents intermediate water before transport to ventilation areas on the Northern Shelf (orange, filled circles, this study); and Station 72 monitors OSIW path "downstream" of ventilation area before export into the North Pacific (blue, filled squares, this study). Station 40N (24) represents final water mix in a southerly position near Kuroshio-Oyashio Extension Region (green, open squares), where new NPIW is formed. Note gradient among WSAPW, OSIW before and after ventilation, and resulting change in NPIW (intermediate water core layer: light blue shaded area). Stations 14/29/84, 110, and 12 (yellow dots in *A*) indicate additional bottom water and surface sediment sample locations used for validation of modern $\delta^{13}C$ characteristics of the epibenthic foraminifer *C. mundulus* (*SI Appendix*, Table S1).

(52°47.272′ N, 144°57.318′ E; 1,082 m water depth) complements the records with a deeper location at the lower boundary of OSIW. Based on an accelerator mass spectrometry (AMS) ^{14}C-anchored stratigraphic framework (*SI Appendix*, *Age Models and Stratigraphic Framework* and Fig. S2), these cores yield sedimentation rates between 20 and 180 cm/ka, thus allowing for the reconstruction of millennial-scale changes in intermediate water ventilation.

Changes in $\delta^{13}C$ for deeper water masses without contact with surface ocean and atmosphere become linearly correlated to regenerated nutrient and O_2 concentrations (21, 22). While in some oceanic regions, other factors alter this relationship (e.g., air–sea exchange processes, thermodynamic effects, or water mass mixing) (22, 23), in the Okhotsk Sea and North Pacific, the $\delta^{13}C$–nutrient–O_2 relationship has been shown to be relatively simple, and these secondary factors play a less important role (24, 25) under the considerations we follow here (*SI Appendix*, Figs. S1 and S2). To validate that heavier $\delta^{13}C$ signatures represent better-ventilated OSIW compared to WSAPW, we measured water-column $\delta^{13}C_{DIC}$ (dissolved inorganic carbon) depth profiles from two stations near our inflow and outflow locations (Fig. 1). Compared with existing North Pacific data (14, 24), we identified about 0.2 to 0.3‰ higher $\delta^{13}C_{DIC}$ values in the OSIW outflow (Station LV29-72-4) than WSAPW mean values of about −0.5‰ (Station HS29, Fig. 1*B*), corroborating our use of $\delta^{13}C$ as proxy for mid-depth water mass ventilation (see *SI Appendix*, *Use of Stable Carbon Isotopes for Assessing OSIW/NPIW Ventilation*).

Before using down-core records for our OSIW reconstructions, we also tested the assumption that epibenthic foraminifera of the genus *C. mundulus* are reliably recording $\delta^{13}C$ of bottom water DIC and do not incorporate unidentified offsets as reported from other oceanic regions and time intervals (18). Our results from eight undisturbed sediment surface sites with corresponding bottom water $\delta^{13}C_{DIC}$ measurements within the Okhotsk Sea show that the $\delta^{13}C$ of live (rose bengal-stained) *C. mundulus* mirrors the $\delta^{13}C$ of bottom waters within ∼0.1‰, which is within commonly accepted values for intrasample variability in benthic foraminifera (*SI Appendix*, Table S1).

A Middle-Holocene Threshold in OSIW Ventilation. The Sakhalin margin cores that monitor OSIW (sites 4, 78, and 79) are characterized by high-amplitude variations throughout the Holocene, exceeding glacial–interglacial changes in Pacific Deep Water ventilation (14), with values between −0.8‰ and −0.1‰ and a close resemblance between single cores. Sample resolution in the deeper core 79 is slightly worse due to the partial absence of *Cibicidoides* species from the benthic fauna; however, core 79's overall $\delta^{13}C$ pattern matches that of the other cores. In contrast, the Kamchatka margin core 108, representing WSAPW inflow, shows $\delta^{13}C$ values ranging mostly between −0.2‰ and −0.5‰, similar to modern values (25) but with no discernible long-term trend over the Holocene (Fig. 2*B*). For better comparison hereafter, we discuss principal characteristics of OSIW based on a combined record (named C-OSIW) of the three outflow, or "downstream" sites representing the OSIW (sites 4, 78, and 79) (Figs. 2 *C*–*E* and 3*A*). We stacked individual records on their own age models into one record and added a 25-point smoothing to the original data to highlight millennial-scale changes (Fig. 3*A*).

Our C-OSIW $\delta^{13}C$ record shows a subdivision of the Holocene into two periods that have differing ventilation patterns (Figs. 2 and 3*A*). The EMH (11 to 6 ka) exhibits significantly lower than modern $\delta^{13}C$ values (Figs. 2 and 3*A*), suggesting persistent ventilation minima in OSIW. In contrast, Late Holocene (LH) (0–6 ka) ventilation increases after a sudden shift around 6 ka (Fig. 2 *C* and *D*) toward modern conditions, featuring a principal Middle-Holocene threshold (or "tipping point") in NPIW ventilation. In addition, the LH (Fig. 3*A*) shows a slight but more gradual increase in the C-OSIW stack toward modern values of $\delta^{13}C$ over the last 1 to 2 ka of about 0.1‰ (Figs. 2 *C* and *D* and 3*A*). Therefore, a critical initial observation of this C-OSIW ventilation reconstruction is that the subarctic North Pacific middepth water layer rapidly changed its characteristics during the Middle Holocene around 6 ka toward the present-day OSIW and the connected mesopelagic North Pacific ventilation prevalence. For a better comparison between the OSIW outflow site (cores 4, 78, and 79) and the WSAPW inflow site (core 108), we subtracted the latter from our C-OSIW record to create a $\Delta\delta^{13}C$ time series (Fig. 3*F*), after resampling our data in evenly spaced 50-y intervals. Our $\Delta\delta^{13}C$ data (Fig. 3*F*) reveal that OSIW ventilation decreased below values of its precursor WSAPW before the 6-ka shift. This negative OSIW–WSAPW gradient (Fig. 3*F*) implies that OSIW export into the North Pacific was, in effect, not actively ventilated in the Okhotsk Sea before 6 ka.

We assume that under Holocene boundary conditions, the principles of OSIW formation through seasonal sea ice, polynya-induced brine rejection, and mixing between surface waters and WSAPW remained essentially similar. However, apparently, the intensity of mixing well-ventilated waters into middepth levels must have increased after the Middle Holocene toward the modern setting. Other processes like changed air–sea exchange or simple source water mass variations (e.g., through higher contributions of Pacific Deep Water or mixed layer water, respectively) cannot fully explain the large observed changes in absolute $\delta^{13}C$ values on millennial timescales, and particularly the EMH negative $\Delta\delta^{13}C$ gradient (*SI Appendix*, Fig. S10). Earlier qualitative multiproxy studies of nearby sites in the Okhotsk Sea (17) showed oceanographic reorganizations around 6 ka. In those results, independent evidence from microfossil assemblages suggested higher mesopelagic productivity with increased microbial biomass and higher organic matter respiration in OSIW before 6 ka (see *SI Appendix*, *Previous Studies Indicating Okhotsk Sea Ventilation Changes*), while support for reduced formation of OSIW and intensified OMZ conditions was also found in nearby sites (17, 26, 27). As a result, we

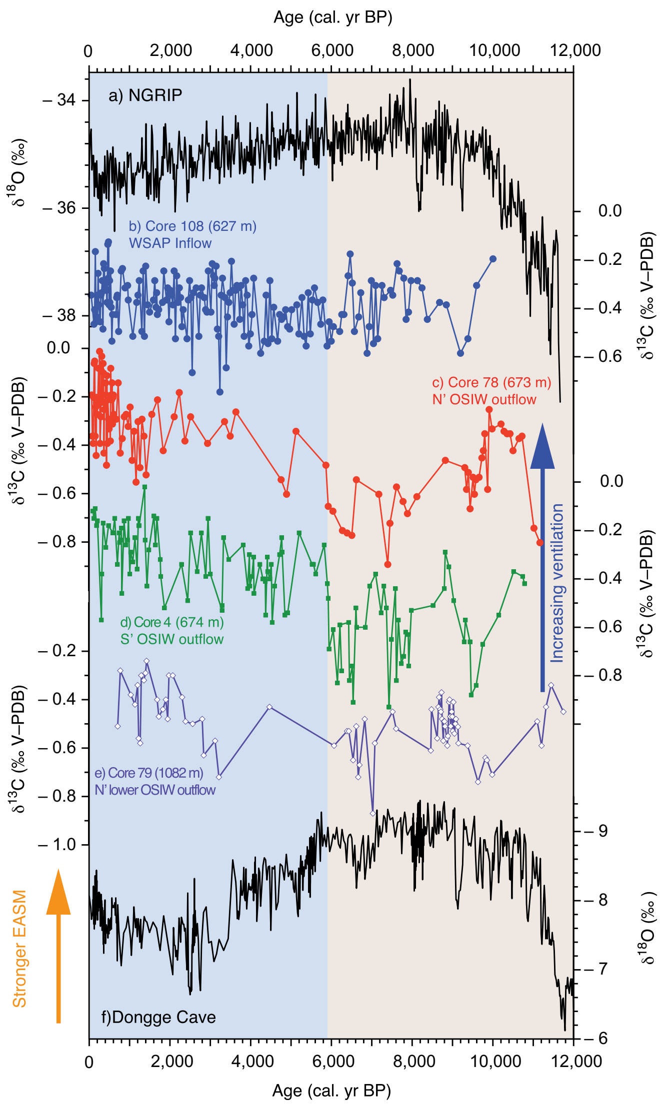

Fig. 2. Stable isotope records of studied cores indicating changes in OSIW ventilation in relation to reference records. (*A*) NGRIP ice core δ^{18}O time series (63). (*B*) Kamchatka margin core 108 epibenthic δ^{13}C, indicating WSAP water inflow. (*C–E*) Sakhalin margin cores epibenthic δ^{13}C, indicating changes in OSIW ventilation: (*C*) core 78 from shallow N Sakhalin margin, (*D*) core 4 from shallow middle Sakhalin margin, and (*E*) core 79 from lower N Sakhalin margin, as labeled. (*F*) Dongge Cave speleothem δ^{18}O time series, representing changes in Southeast Asian summer monsoon and links to North Atlantic climate (29). Colored background highlights the two different main ventilation phases from 0 to 6 ka (LH) and from 6 to 11 ka (EMH).

presume that during the EMH, physical processes likely inhibited the modern ventilation scheme, while increased remineralization of organic matter through respiration within the mixed layer and in OSIW decreased the ventilation of OSIW relative to WSAPW entering the Okhotsk Sea, leading to higher inventories of nutrients and carbon in NPIW.

Connection to Pacific and Northern Hemisphere Holocene Climate. To explain the forcing behind the observed variations in OSIW ventilation, and in particular the Middle-Holocene climatic shift toward the modern well-ventilated regime, we compared our data to other regional records. Globally, and in regions influenced by the East Asian summer monsoon (EASM) (Figs. 2*F* and 4*B*), a Middle-Holocene shift is documented (28). Before 6 ka, a stronger EASM (29, 30) propagated further northeastward than at present, yielding higher precipitation and temperatures in the Okhotsk Sea hinterland (31), increasing runoff from the Amur River catchment into the Okhotsk Sea (32). Higher Amur freshwater discharge also transports significant amounts of heat to the Okhotsk Sea (32, 33), which suppresses sea ice formation and, in concert with stronger thermal stratification of the upper mixed layer (34), decreases OSIW ventilation. After 6 ka, strengthening and expansion of the winter Siberian High in concert with a southward retreating EASM front was likely responsible for strengthening cold northeasterly winds over the continental shelf region (35). In addition, the maximum sea ice extent in the Okhotsk Sea is dependent on mean sea surface temperature (SST) conditions in summer (36). We thus infer a longer and more extensive sea ice cover, more polynyas, and more vigorous mixing of the mixed layer after 6 ka, which together enhanced the ventilation of new OSIW.

Alkenone-derived SSTs for the Okhotsk Sea and the Japan continental margin consistently show maxima in Holocene SSTs between ~8 and 6 ka, decreasing SSTs between 6 and 4 ka, and a last shift toward persistent colder SSTs around 2 ka (37, 38) (Fig. 3*D*). Our observed decrease in OSIW ventilation during the EMH is thus in close agreement with increased SSTs of about 1.5 to 2 °C derived from both regional and global reconstructions (38, 39). Importantly, recent low-latitude middepth thermocline temperature changes (at around 500 m water depth) in the equatorial West Pacific show concomitant higher temperatures in the EMH of similar magnitude, with northern NPIW-sourced thermocline or intermediate water temperatures (Fig. 3*C*) being warmer by 2.1 ± 0.4 °C than during the last century (40), in strong accord with our assumed decrease in ventilation in OSIW and NPIW (Fig. 3 *A* and *F*).

Results from Earth System Model COSMOS (Community Earth System Model) simulations corroborate our proxy-based assumptions. This model captures the modern physical characteristics of NPIW well under preindustrial (PI) conditions (*SI Appendix*, Fig. S5 *A* and *C*). We analyzed Pacific data from PI and 9-ka time-slice runs (for details, see *SI Appendix*, *Paleoclimate Modeling* and ref. 41). On a meridional transect along 150° E through the Okhotsk Sea toward the equatorial Pacific, our model results show a consistently warmer (around 1 to 2 °C) and saltier intermediate water layer at 9 ka than at PI conditions (Fig. 4 *A* and *B* and *SI Appendix*, Fig. S5 *B* and *D*), matching the proxy-based temperature changes surprisingly well (40). Model-derived anomalies (9 ka minus PI) in sea ice dynamics show a localized, significant decrease of both sea ice volume (Fig. 4*C*) and thickness (Fig. 4*D*) in the Okhotsk Sea in the EMH, in agreement with our hypothesized reductions in sea ice and polynya formation in the OSIW source region that inhibited the modern ventilation regime.

Millennial-Scale Variations in Middepth Ventilation. Superimposed on the described stepwise background changes, we detected distinct cyclic millennial-scale variations in OSIW ventilation, visible in the δ^{13}C C-OSIW ventilation record (Fig. 3*A*) and in wavelet analyses of both the combined and individual records (*SI Appendix*, Figs. S7–S9). These variations occur in the range of 1,500 to 1,800 y, which have been reported from a number of locations and Holocene proxy records (42, 43). Notably, this cyclicity is most prominent before the Middle-Holocene tipping point (28). While other records yielded comparable changes in terrestrial and surface ocean records, which were attributed to either internal (43) or external [e.g., solar (44)] forcing, evidence for a direct connection to middepth and deep water formation or ventilation patterns, such as we observe here, has remained relatively scarce to date (28, 42). Thus, our record provides evidence for the close link between high- to midlatitude surface ocean processes (SST and stratification changes) and intermediate water ventilation dynamics on Holocene millennial (and potentially shorter) timescales.

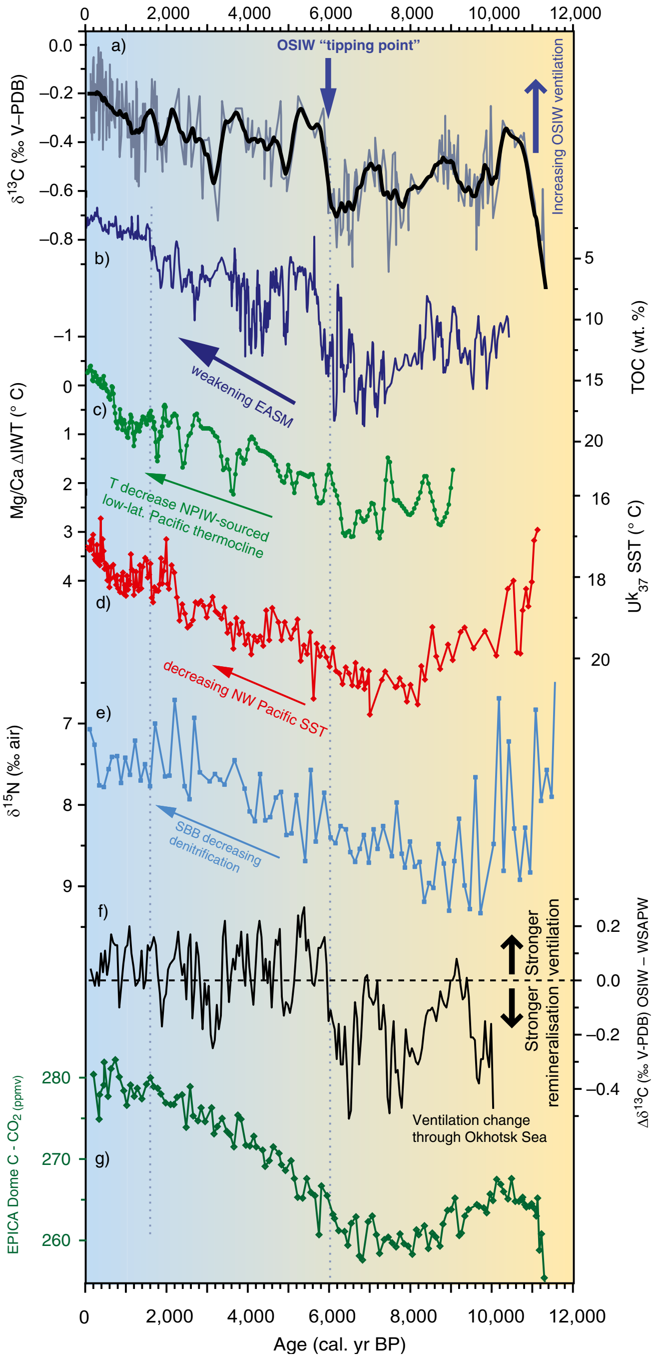

Fig. 3. OSIW ventilation dynamics and gradients compared with long-term changes in regional and global climate records. (*A*) $\delta^{13}C_{OSIW}$ combined record of sites 4, 78, and 79, indicating OSIW ventilation dynamics. Gray line: original data; black thick line: resampled 25-point moving average. (*B*) Proxy record for intensity of EASM changes in Huguangyan Maar Lake, southern China, as expressed in total organic carbon (TOC) content (30). Note inverted scale for better comparison with OSIW ventilation record. (*C*) Reconstruction of intermediate water temperature (IWT) (inverted) in the equatorial West Pacific at 500 m water depth, indicative of northern-sourced NPIW reaching the low-latitude thermocline. Calculated changes over the Holocene with reference to the last 100 y, based on Mg/Ca ratios of benthic foraminifera (40). (*D*) Composite alkenone-based high-resolution SST record from Japan margin (cores MD01-2421, KR02-06_MC, and KR02-06_GC) (38). (*E*) NE Pacific Santa Barbara Basin (SBB) $\delta^{15}N_{bulk}$ record, indicating denitrification and nutrient utilization changes in waters under NPIW influence (55). (*F*) Ventilation difference between OSIW and WSAPW, expressed as $\Delta\delta^{13}C$ between the stacked C-OISW record and site 108 (this study). Positive values (above dashed "zero" line) denote active ventilation in the Okhotsk Sea; negative values indicate ventilation loss in the Okhotsk Sea due to remineralization processes and lack of new water mass formation. (*G*) Atmospheric CO_2 record from EPICA Dome C ice core record (64).

In the subarctic Pacific, other evidence for Holocene millennial-scale cycles in marine sequences is scarce; however, a southerly located Japan margin SST record (38) also showed 1,500-y cycles in SST anomalies (see original data of ref. 38 in Fig. 3*D*). A northward propagation of low-latitude warm Kuroshio waters would plausibly explain the strong correspondence between Japan offshore SST records and Okhotsk Sea decreases in ventilation due to warming and salinification of upper ocean water masses (38), as well as the closer coupling between the midlatitude North Pacific and the subarctic Okhotsk Sea region. For future warming scenarios, such a pattern has been observed in recent modeling results, which indicated an intensification and northward shift of most Western Boundary Currents (45). As the 1,500-y variations are most prominent during the EMH in our records, we presume that during periods of suppressed OSIW ventilation, this modulation via oceanic forcing and the global Meridional Overturning Circulation gains importance.

High-Latitude Mesopelagic Oxygenation and Remineralization Changes: Effects and Feedbacks. In principle, benthic $\delta^{13}C$ may, in addition, provide qualitative information on past baseline variations of bottom water oxygenation (46, 47) (see *SI Appendix*, *Estimation of Past Oxygenation Based on* $\delta^{13}C$ *Isotope Values*). However, because O_2 in seawater equilibrates with the atmosphere almost instantaneously (i.e., on timescales of a year or less), whereas DIC and its carbon isotopes react on timescales of a decade [i.e., with about an order of magnitude difference (48)], only long-term, millennial-scale changes can be inferred. Correlation between dissolved water column O_2 and $\delta^{13}C_{DIC}$ based on water column data from the Okhotsk Sea (*SI Appendix*, Figs. S3 and S4) can thus provide some insight into potential ranges of past Holocene middepth oxygenation levels. When applying this modern relationship between O_2 and $\delta^{13}C$ to assess long-term oxygenation changes for OSIW, the last 0 to 6 ka would broadly range within modern instrumental data, indicating a moderately oxic environment (i.e., 100 to 200 μmol/L ± 50 μmol/L) (2, 3). In contrast, O_2 estimates for the preceding EMH interval, before the 6-ka threshold, show oxygenation levels that did not reach even the lower range of modern O_2 concentrations (*SI Appendix*, Figs. S3 and S4). EMH O_2 values would have mostly yielded just 30 to 50% of modern ranges (50 to 120 μmol/L ± 50 μmol/L) and thus imply a substantial reduction in oxygenation of middepth waters. Taken at face value, OSIW oxygen supply would have been significantly reduced in a warmer-than-present EMH, changing the Okhotsk Sea from a modern mesopelagic O_2 source into an episodically hypoxic sink before 6 ka (*SI Appendix*, Fig. S4), with likely limitations for marine life, OMZ strengthening (49, 50), and altered biogeochemical nutrient cycles (51, 52). This largely qualitative assessment, while not without methodological caveats like most proxy-based assessments of paleooxygenation levels (53, 54), is in agreement with synthesis results indicating an expansion of Early-Holocene OMZs on both a global scale and in the middepth Indo-Pacific (54). Also, independent evidence based on benthic foraminiferal assemblage analyses and multiproxy records recently indicated intensifications of O_2-limited conditions in both the subarctic Northwest (27) and the Northeast Pacific, with more dysoxic conditions during the EMH (55, 56) (Fig. 3*E*).

Modern NPIW provides nutrients, in particular silicate and phosphate, to lower latitudes via the "ocean tunnel" mechanism—that is, the meridional export of entrained nutrients in intermediate

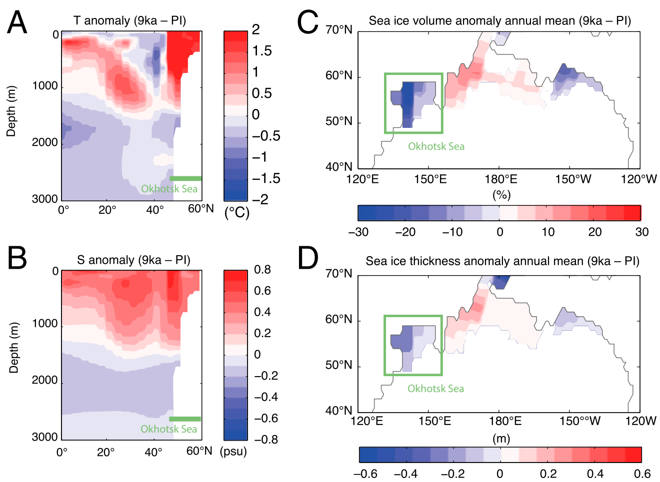

Fig. 4. Model results from the earth system model COSMOS. Results are plotted in all panels as anomalies, calculated as differences resulting from 9 ka minus PI runs. (*A*) Annual mean temperature (T) anomaly, shown on a meridional transect along 150° E from the equator to 60° N. The transect crosses directly into the Okhotsk Sea north of 42° N. (*B*) Same as in *A* but for annual mean salinity (S) anomaly. (*C*) Sea ice volume anomaly 9 ka minus PI, calculated from sea ice concentration multiplied by sea ice thickness in the North Pacific. (*D*) Same as *C*, but for sea ice thickness.

waters to subtropical and equatorial Pacific thermocline waters that are nutrient limited (57). Currently, nutrient limitation in these low-latitude regions hampers their efficiency of new and export biological production and the resulting sequestration of carbon to the deep ocean via the "biological carbon pump." Thus, the modern low-latitude Pacific is one of the largest CO_2 source regions to the atmosphere. Today, while only about one-third of water reaching the equatorial thermocline is estimated to stem from NPIW, it provides about two-thirds of silicate and other nutrients needed to sustain biosiliceous primary production in the low-latitude Pacific (58, 59). On glacial–interglacial timescales, this nutrient transport might have increased during cold time intervals (60, 61). We suggest that, in the Holocene as well, NPIW export acted as a feedback mechanism on the biological carbon pump and thus atmospheric CO_2 (*i*) through intensification and deepening of remineralization processes, thereby storing higher amounts of organic carbon in North Pacific middepth waters; and (*ii*) by exporting larger amounts of nutrients, in particular silicate, through OSIW and NPIW to lower-latitude thermocline waters, thus attenuating silicate limitation in the northern subtropical-to-equatorial Pacific during warmer-than-present Holocene phases (Fig. 3 *D* and *E*). This latter process is supported by evidence for higher nutrient concentrations and utilization in the western equatorial Pacific and its subtropical marginal seas during the EMH that are currently under the influence of NPIW inflow (61) and concurrent minima in atmospheric CO_2 concentrations (Fig. 3*G*).

In summary, our combined proxy- and modeling-based reconstructions show a crucial influence of Okhotsk Sea-sourced NPIW on Pacific Holocene oceanography. In particular, export of warmer, oxygen-poorer, and nutrient-richer NPIW from the subarctic domain likely reached and influenced the low-latitude Pacific thermocline during the warmer-than-present EMH, thus not only leading to increases in oceanic heat content (40), but also to significant changes in the biogeochemical signatures of thermocline waters, including equatorial Pacific nutrient and oxygen inventories (12, 52).

Conclusions

Our study highlights the nonlinear behavior of North Pacific middepth waters on millennial timescales under past, warmer-than-present climate conditions. We show that the modern NPIW ventilation pattern, as reconstructed from high-resolution $\delta^{13}C$ records from the Okhotsk Sea, has only been prevalent since about 1 to 2 ka, while little to no ventilation prevailed for most of the warmer EMH. Millennial-scale variations in OSIW ventilation occur superimposed on these long-term baseline ventilation adjustments, with a main cyclicity of 1,500 to 1,800 y, indicating a relation of our dominant forcing factors to globally observed internal oscillation dynamics of ocean overturning.

A comparison between subarctic Pacific Gyre source waters and intermediate water exported from the Okhotsk Sea over the last 11 ka implies that a threshold occurred at 6 ka and rapidly changed NPIW characteristics from a remineralization-dominated high-nutrient inventory to the modern regime of relatively better-ventilated middepth waters. Accordingly, we hypothesize that before 6 ka, NPIW was exporting higher amounts of nutrients, especially silicate, to nutrient-limited subtropical-to-equatorial Pacific thermocline waters via ocean tunneling, potentially providing a feedback mechanism that enhanced new biosiliceous production and thus the efficiency of the biological carbon pump during the EMH.

Based on the composite $\delta^{13}C$ record of OSIW we also estimate that average middepth NPIW oxygen concentrations during the EMH were likely lower by 25 to 50% than they are today, which would have led to near-hypoxic conditions in the modern source region of North Pacific ventilation. Starting around 6 ka, the Okhotsk Sea switched from an EMH ventilation deficiency to the modern oxygenated regime, seemingly in lockstep with thermocline (500 m) temperature declines in the low-latitude equatorial Pacific and decreases in high-latitude Northwest Pacific SSTs.

As future global SSTs are thought to resemble or surpass Early-Holocene SST values (39), significant changes toward lower ventilation of middepth waters and thus O_2 supply from subarctic latitudes, coupled with changed ventilation feedback mechanisms, may be expected for the middepth Pacific. These will likely affect oxygen- and nutrient-dependent biogeochemical cycles in the lower latitudes. Given the significant importance of intermediate water masses in the Pacific Ocean and their short response time within years or decades to changing environmental forcing (2), further studies should try to elucidate the role of intermediate waters in influencing global marine nutrient, oxygen, and carbon budgets during warmer-than-modern times like the Early Holocene, which at present remain inadequately understood.

Methods

To reconstruct changes in ventilation patterns of middepth water masses, we used the stable carbon isotopic composition ($\delta^{13}C$) of benthic foraminiferal *C. mundulus* tests. Samples were measured on a Thermo Finnigan MAT 252 mass spectrometer coupled online to a Kiel CARBO II unit, and $\delta^{13}C$ of seawater DIC values were measured on a Thermo Finnigan Delta E with an automated DICI-II preparation unit (see *SI Appendix, Site Selection – Material and Methods* for details). All values are reported in δ notation vs. Vienna Pee Dee Belemnite (‰ V-PDB).

Age control for cores 4 and 79 has been previously reported in detail (62). Age control for cores 78 and 108 was achieved through six and nine AMS ^{14}C dates, respectively, of planktic foraminifera (*SI Appendix*, Figs. S4 and S5). Methodology for construction of age models for all cores and age-depth relationships for cores 78 and 108 are provided in detail in *SI Appendix, Age Models and Stratigraphic Framework* and Figs. S4–S6.

ACKNOWLEDGMENTS. We thank the masters and crews of the research vessel Akademik M.A. Lavrentyev during cruises LV28 and LV29 for their support; S. Fessler, N. Stange, A. Kaiser, and L. Haxhiaj for help in sample preparation and laboratory support; and two anonymous reviewers for their thoughtful comments that significantly helped to improve the manuscript. This study was funded through the Kurile-Okhotsk Sea Marine Experiment (KOMEX I and II) projects and the Sino-German Pacific–Arctic Experiment (SiGePAX) project (Grant 03F0704A) by the German Ministry of Education and Research, with additional financial support by the Alfred-Wegener-Institut and the Helmholtz Climate Initiative REKLIM (Regionale Klimaänderungen).

1. Emerson S, Watanabe YW, Ono T, Mecking S (2004) Temporal trends in apparent oxygen utilization in the upper pycnocline of the North Pacific: 1980–2000. *J Oceanogr* 60:139–147.
2. Nakanowatari T, Ohshima KI, Wakatsuchi M (2007) Warming and oxygen decrease of intermediate water in the northwestern North Pacific, originating from the Sea of Okhotsk, 1955-2004. *Geophys Res Lett* 34:L04602.
3. Whitney FA, Freeland HJ, Robert M (2007) Persistently declining oxygen levels in the interior waters of the eastern subarctic Pacific. *Prog Oceanogr* 75:179–199.
4. Kwon EY, Deutsch C, Xie S-P, Schmidtko S, Cho Y-K (2016) The North Pacific oxygen uptake rates over the past half century. *J Clim* 29:61–76.
5. Warren B (1983) Why is no deep water formed in the North Pacific? *J Mar Res* 41: 327–347.
6. Talley LD (1985) Ventilation of the sub-tropical North Pacific: The shallow salinity minimum. *J Phys Oceanogr* 15:633–649.
7. Reid JL (1965) Intermediate waters of the Pacific Ocean. *The Johns Hopkins Oceanographic Studies* (Johns Hopkins Univ Press, Baltimore), pp 1–85.
8. Shcherbina AY, Talley LD, Rudnick DL (2003) Direct observations of North Pacific ventilation: Brine rejection in the Okhotsk Sea. *Science* 302:1952–1955.
9. Talley LD (1993) Distribution and formation of North Pacific intermediate water. *J Phys Oceanogr* 23:517–537.
10. Ito T, Deutsch CA (2013) Variability of the oxygen minimum zone in the tropical North Pacific during the late twentieth century. *Global Biogeochem Cycles* 27:1119–1128.
11. Keeling RE, Körtzinger A, Gruber N (2010) Ocean deoxygenation in a warming world. *Annu Rev Mar Sci* 2:199–229.
12. Gilly WF, Beman JM, Litvin SY, Robison BH (2013) Oceanographic and biological effects of shoaling of the oxygen minimum zone. *Annu Rev Mar Sci* 5:393–420.
13. Hill K, Weaver A, Freeland H, Bychkov A (2003) Evidence of change in the Sea of Okhotsk: Implications for the North Pacific. *Atmos -Ocean* 41:49–63.
14. Keigwin L (1998) Glacial-age hydrography of the far northwest Pacific Ocean. *Paleoceanography* 13:323–339.
15. Gorbarenko SA, et al. (2012) Responses of the Okhotsk Sea environment and sedimentology to global climate changes at the orbital and millennial scale during the last 350 kyr. *Deep Sea Res Part II: Top Stud Oceanogr* 61–64:73–84.
16. Itaki T, Ikehara K (2004) Middle to Late Holocene changes of the Okhotsk Sea intermediate water and their relation to atmospheric circulation. *Geophys Res Lett* 31: L24309.
17. Gorbarenko SA, et al. (2010) Paleoenvironment changes in the NW Okhotsk Sea for the last 18 kyr determined with micropaleontological, geochemical, and lithological data. *Deep Sea Res Part I Oceanogr Res Pap* 57:797–811.
18. Gottschalk J, et al. (2016) Carbon isotope offsets between benthic foraminifer species of the genus *Cibicides* (*Cibicidoides*) in the glacial sub-Antarctic Atlantic. *Paleoceanography* 31:1583–1602.
19. Biebow N, Kulinich R, Baranov B,eds. (2002) KOMEX II, Kurile Okhotsk Sea Marine Experiment: Cruise report RV Akademik M.A.Lavrentyev cruise 29, Leg 1 and Leg 2: Vladivostok - Pusan - Okhotsk Sea - Pusan - Okhotsk Sea - Pusan - Vladivostok; May 25 - August 05, 2002 [BMBF contract 03G0568 A - Joint project no. 01020094]; GEOMAR-Report, 110. (GEOMAR Forschungszentrum für Marine Geowissenschaften Kiel, Kiel, Germany), p. 190.
20. Biebow N, Hütten E, eds. (1999) KOMEX: Kurile Okhotsk Sea Marine Experiment Cruise Reports: KOMEX I and II; RV Professor Gagarinsky Cruise 22, RV Akademik M. A. Lavrentyev Cruise 28: Vladivostok - Pusan - Okhotsk Sea - Pusan - Vladivostok, 7 July - 12 September 1998. GEOMAR-Report, 082. (GEOMAR Forschungszentrum für marine Geowissenschaften der Christian-Albrechts-Universität zu Kiel, Kiel, Germany), p. 188.
21. Kroopnick PM (1985) The distribution of ^{13}C of $\sum CO_2$ in the world oceans. *Deep Sea Res Part I Oceanogr Res Pap* 32:57–84.
22. Hoogakker BAA, Thornalley DJR, Barker S (2016) Millennial changes in North Atlantic oxygen concentrations. *Biogeosciences* 13:211–221.
23. Lynch-Stieglitz J, Stocker TF, Broecker WS, Fairbanks RG (1995) The influence of air-sea exchange on the isotopic composition of oceanic carbon: Observations and modeling. *Global Biogeochem Cycles* 9:653–665.
24. Itou M, Ono T, Noriki S (2003) Provenance of intermediate waters in the western North Pacific deduced from thermodynamic imprint on delta C-13 of DIC. *J Geophys Res Oceans* 108:3347.
25. Bauch D, Erlenkeuser H, Winckler G, Pavlova G, Thiede J (2002) Carbon isotopes and habitat of polar planktic foraminifera in the Okhotsk Sea: The 'carbonate ion effect' under natural conditions. *Mar Micropaleontol* 45:83–99.
26. Gorbarenko SA, et al. (2007) Millennium scale environment changes of the Okhotsk Sea during last 80 kyr and their phase relationship with global climate changes. *J Oceanogr* 63:609–623.
27. Bubenshchikova NV, Nuernberg D, Gorbarenko SA, Lembke-Jene L (2010) Variations of the oxygen minimum zone of the Okhotsk Sea during the last 50 ka as indicated by benthic foraminiferal and biogeochemical data. *Okeanologiya* 50:93–106.
28. Debret M, et al. (2009) Evidence from wavelet analysis for a mid-Holocene transition in global climate forcing. *Quat Sci Rev* 28:2675–2688.
29. Dykoski C, et al. (2005) A high-resolution, absolute-dated Holocene and deglacial Asian monsoon record from Dongge Cave, China. *Earth Planet Sci Lett* 233:71–86.
30. Shen J, et al. (2013) Ti content in Huguangyan Maar Lake sediment as a proxy for monsoon-induced vegetation density in the Holocene. *Geophys Res Lett* 40: 5757–5763.
31. Bazarova VB, Mokhova LM, Klimin MA, Kopoteva TA (2011) Vegetation development and correlation of Holocene events in the Amur River basin, NE Eurasia. *Quat Int* 237: 83–92.
32. Tachibana Y, Oshima K, Ogi M (2008) Seasonal and interannual variations of Amur River discharge and their relationships to large-scale atmospheric patterns and moisture fluxes. *J Geophys Res D Atmospheres* 113:D16102.
33. Ogi M, Tachibana Y, Nishio F, Danchenkov M (2001) Does the fresh water supply from the Amur River flowing into the sea of Okhotsk affect sea ice formation? *J Meteorol Soc Jpn* 79:123–129.
34. Riethdorf J-R, Max L, Nürnberg D, Lembke-Jene L, Tiedemann R (2013) Deglacial history of (sub) sea surface temperatures and salinity in the subarctic NW Pacific: Implications for upper-ocean stratification. *Paleoceanography* 28:91–104.
35. Harada N, et al. (2014) Holocene sea surface temperature and sea ice extent in the Okhotsk and Bering seas. *Prog Oceanogr* 126:242–253.
36. Nakanowatari T, Ohshima KI, Nagai S (2010) What determines the maximum sea ice extent in the Sea of Okhotsk? Importance of ocean thermal condition from the Pacific. *J Geophys Res Oceans* 115:C12031.
37. Max L, et al. (2012) Sea surface temperature variability and sea-ice extent in the subarctic northwest Pacific during the past 15,000 years. *Paleoceanography* 27: PA3213.
38. Isono D, et al. (2009) Sea surface temperature reconstruction of a combined sediment record of the midlatitude North Pacific. *PANGAEA*, 10.1594/PANGAEA.841034.
39. Marcott SA, Shakun JD, Clark PU, Mix AC (2013) A reconstruction of regional and global temperature for the past 11,300 years. *Science* 339:1198–1201.
40. Rosenthal Y, Linsley BK, Oppo DW (2013) Pacific Ocean heat content during the past 10,000 years. *Science* 342:617–621.
41. Wei W, Lohmann GP (2012) Simulated Atlantic multidecadal oscillation during the Holocene. *J Clim* 25:6989–7002.
42. Wirtz KW, Lohmann G, Bernhardt K, Lemmen C (2010) Mid-Holocene regional reorganization of climate variability: Analyses of proxy data in the frequency domain. *Palaeogeogr Palaeoclimatol Palaeoecol* 298:189–200.
43. Debret M, et al. (2007) The origin of the 1500-year climate cycles in Holocene North-Atlantic records. *Clim Past* 3:569–575.
44. Bond G, et al. (2001) Persistent solar influence on North Atlantic climate during the Holocene. *Science* 294:2130–2136.
45. Yang H, et al. (2016) Intensification and poleward shift of subtropical western boundary currents in a warming climate. *J Geophys Res Oceans* 121:4928–4945.
46. Schmiedl G, Mackensen A (2006) Multispecies stable isotopes of benthic foraminifers reveal past changes of organic matter decomposition and deepwater oxygenation in the Arabian Sea. *Paleoceanography* 21:PA4213.
47. Hoogakker BAA, Elderfield H, Schmiedl G, McCave IN, Rickaby REM (2015) Glacial-interglacial changes in bottom-water oxygen content on the Portuguese margin. *Nat Geosci* 8:40–43.
48. Schmittner A, et al. (2013) Biology and air–sea gas exchange controls on the distribution of carbon isotope ratios (δ13C) in the ocean. *Biogeosciences* 10:5793–5816.
49. Stramma L, et al. (2011) Expansion of oxygen minimum zones may reduce available habitat for tropical pelagic fishes. *Nat Clim Chang* 2:33–37.
50. Karstensen J, Stramma L, Visbeck M (2008) Oxygen minimum zones in the eastern tropical Atlantic and Pacific oceans. *Prog Oceanogr* 77:331–350.
51. Kwon EY, Primeau F, Sarmiento JL (2009) The impact of remineralization depth on the air–sea carbon balance. *Nat Geosci* 2:630–635.
52. Deutsch C, Brix H, Ito T, Frenzel H, Thompson L (2011) Climate-forced variability of ocean hypoxia. *Science* 333:336–339.
53. Jaccard SL, Galbraith ED, Frölicher TL, Gruber N (2014) Ocean (de)oxygenation across the last deglaciation: Insights for the future. *Oceanography* 27:26–35.
54. Jaccard SL, Galbraith ED (2012) Large climate-driven changes of oceanic oxygen concentrations during the last deglaciation. *Nat Geosci* 5:151–156.
55. Emmer E, Thunell RC (2000) Nitrogen isotope variations in Santa Barbara Basin sediments: Implications for denitrification in the eastern tropical North Pacific during the last 50,000 years. *Paleoceanography* 15:377–387.
56. Ohkushi K, et al. (2013) Quantified intermediate water oxygenation history of the NE Pacific: A new benthic foraminiferal record from Santa Barbara basin. *Paleoceanography* 28:453–467.
57. Sarmiento JL, Gruber N, Brzezinski MA, Dunne JP (2004) High-latitude controls of thermocline nutrients and low latitude biological productivity. *Nature* 427:56–60.
58. Dugdale RC, et al. (2002) Meridional asymmetry of source nutrients to the equatorial Pacific upwelling ecosystem and its potential impact on ocean–atmosphere CO_2 flux; a data and modeling approach. *Deep Sea Res Part II Top Stud Oceanogr* 49: 2513–2531.
59. Dugdale RC, Wilkerson FP, Minas HJ (1995) The role of a silicate pump in driving new production. *Deep Sea Res Part I Oceanogr Res Pap* 42:697–719.
60. Max L, et al. (2017) Evidence for enhanced convection of North Pacific intermediate water to the low-latitude Pacific under glacial conditions. *Paleoceanography* 32: 41–55.
61. Li D, et al. (2017) Millennial-scale ocean dynamics controlled export productivity in the subtropical North Pacific. *Geology* 45:651–654.
62. Lembke-Jene L, et al. (2017) Deglacial variability in Okhotsk Sea intermediate water ventilation and biogeochemistry: Implications for North Pacific nutrient supply and productivity. *Quat Sci Rev* 160:116–137.
63. Blockley SPE, et al. (2011) Synchronisation of palaeoenvironmental records over the last 60,000 years, and an extended INTIMATE event stratigraphy to 48,000 b2k. *Quat Sci Rev* 36:2–10.
64. Augustin L, et al.; EPICA community members (2004) Eight glacial cycles from an Antarctic ice core. *Nature* 429:623–628.